

## COMPARATIVE STUDY OF ANN AND ANFIS MODELS FOR PREDICTING TEMPERATURE IN MACHINING

SOROUGH MASOUDI<sup>1,\*</sup>, MOHAMMAD SIMA<sup>2</sup>, MAJID TOLOUEI-RAD<sup>3</sup>

<sup>1</sup>Young Researchers and Elite Club, Najafabad Branch,  
Islamic Azad University, Najafabad, Iran

<sup>2</sup>Department of industrial engineering, Lamar University, Beaumont, TX, USA

<sup>3</sup>School of Engineering, Edith Cowan University, Perth, Western Australia

\*Corresponding author: smasoudi86@gmail.com

### Abstract

The Mechanism of heat generation at the cutting region (tool-workpiece interface) during machining processes is a highly complicated phenomenon and depends on many process parameters. Elevated temperature during the machining process is a root cause of residual stress on the machined part as well as a cause of rapid tool wear. Although several methods have been developed to measure the temperature in machining, the in-situ application of these methods has many technical problems and restrictions. As a result, the utilization of computational methods to predict temperature in machining is very demanding. In this paper, the artificial intelligent models known as Artificial Neural Network (ANN) and Adaptive Neuro Fuzzy Inference System (ANFIS) were used to model and predict the temperature in machining. Several experiments were conducted to validate these models. These experiments were carried out on thin-walled AL7075 work pieces to investigate the effect of different machining parameters on temperature in turning. A thermal imaging Infrared (IR) camera was used to measure the temperature of the cutting area during machining. With respect to experimental data, the ANN and ANFIS models were developed and the results obtained from those models were then compared to the experimental results to evaluate the performance of the models. According to the results, the ANFIS model is superior to the ANN model in terms the accurate and reliable prediction of temperature in machining.

Keywords: Turning, Temperature, Infrared measurements, ANN, ANFIS.

### 1. Introduction

In machining, the major portion of consumed energy for metal deformation and also friction between tool and work-piece appears as high heat in the cutting area [1]

**Nomenclatures**

$q_e$	Radiated Energy, J
$T$	Thermo-Dynamical Temperature of the Object, °C
$T_\alpha$	Atmosphere Temperature, °C
$T_r$	Displayed Temperature by the Camera, °C
$T_\mu$	Environment's Temperature, °C

**Greek Symbols**

$\alpha$	Absorptivity
$\sigma$	Stefan Boltzmann Constant, $\frac{w}{M^2K^4}$
$\tau$	Transmissivity
$\varepsilon$	Emissivity Coefficient
$\rho$	Reflectivity

**Abbreviations**

ANFIS	Adaptive Neuro Fuzzy Inference System
ANN	Artificial Neural Network
IR	Infrared Radiation

This generated heat causes numerous economical and technical problems such as rapid tool wear, residual stresses and thermal distortion [2]. Therefore, it is necessary to have a comprehensive understanding of the mechanism of heat generation, intensity, and its distribution in the cutting zone.

Temperature measurement in the cutting area is a challenging task in machining studies. Numerous measurement methods have been developed to measure temperature, such as thermocouple, infrared radiation (IR), the hardness test, and analysis of microstructure changes [3]. One effective technique for temperature measurement in machining is infrared radiation measurement, which is a non-contact method. In this method, the temperature of an object is measured based on the thermal energy or infrared radiation emitted from an object [4]. This technique utilizes an infrared camera to measure the temperature of the cutting area. In order to have a better understanding of this mechanism, its principles will be explained in detail in the next chapter.

Soft computing methods, such as Artificial Neural Network (ANN) and Adaptive Neuro Fuzzy Inference System (ANFIS), have been applied successfully for modelling and predicting machining processes outputs. A broad literature survey was conducted on the application of artificial intelligence systems to predict machining process outputs [5]. Rangwala et al. [6] used neural networks for the prediction of machining performance. The authors applied a feed forward neural network model to predict cutting performance in the turning process. Rai et al. [7] developed a new model to predict the shear plane temperature during end milling by using a feed forward back propagation neural network. The results obtained from their proposed model showed strong agreement with the experimental tests. Korkut et al. [8] utilized a neural network to predict tool-chip interface temperature. In their research, different models were developed that used cutting speed, feed rate, and depth of cut in the end milling process to predict cutting temperature. According to their results, the training

ANN model with the Levenberg-Marquardt (LM) algorithm provides a more accurate prediction of temperature when compared to the trained regression analysis method in machining. Azouzi et al. [9] developed a neural network model to predict surface roughness and dimensional deviation in machining [9]. A neural network-based methodology was utilized by Kohli et al. [10] to predict surface finish in the turning process. They proposed a new methodology for using small training and testing data in their work. Quiza et al. [11] developed a multilayer perceptron neural network model for tool wear prediction in hard turning. They found that the ANN model, in comparison with the regression model, predicts tool wear more accurately.

In addition to ANN, different ANFIS models have been developed to predict machining output parameters in the machining process. Aydin et al. [12] presented an ANFIS model for the prediction of cutting zone temperature in the turning of austenitic stainless steel using multi-layer coated tungsten carbide tools. Their results indicate that the predicted cutting zone temperatures are in strong agreement with the measured temperature. Madić et al. [13] developed an ANN model for prediction of surface roughness in CO<sub>2</sub> laser cutting. According to their results, the ANN could predict the results very accurately. Azami [14] developed an ANFIS model to monitor tool wear using measured machining forces. The model was able to match the nonlinear relationship between tool wear and feed force. To predict surface roughness in grinding, Hamza [15] developed a Multi-objective neural network which, according to their results, is about 91% accurate.

The mechanism of heat generation in cutting areas is a highly complicated phenomenon and depends on many parameters. Although several methods have been developed to measure the temperature in machining, application of these methods presents many technical problems and restrictions. Therefore, the application of soft computing methods in machining is very demanding and can be considered as the novelty of this paper.

The main purpose of this article is to develop and compare the ANN and ANFIS models on how they can predict accurate temperature at the cutting area in machining processes. For this purpose, several experiments were designed and conducted to investigate the effect of different process parameters on temperature in the turning of a thin walled work piece made of AL7075 alloy. With respect to experimental data, the ANN and ANFIS models were developed and the results obtained from those models were then compared to the experimental results to evaluate the performance of the models that can be considered as the novelty of the present work. A thermal imaging infrared camera was used to measure the temperature during machining and the influential factors on the accuracy of the measurements were evaluated so as to get more accurate results.

## 2. Principles of Infrared Temperature Measurement

The Stefan-Boltzmann law describes the power radiated from a black body in terms of its temperature. Specifically, the Stefan-Boltzmann law states that the total energy radiated per unit surface area of a black body across all wavelengths per unit time:

$$q_e = \varepsilon\sigma T^4 \quad (1)$$

where  $q_e$  is the radiated energy,  $T$  is the absolute temperature,  $\sigma$  is the Stefan Boltzmann constant and is equivalent to  $5.67 \times 10^{-8} \left(\frac{W}{M^2K^4}\right)$  and  $\varepsilon$  is the emissivity coefficient.

Emissivity is the measure of an object's ability to emit infrared energy. Emissivity can have a value from 0 (shiny mirror) to 1.0 (blackbody) [16]. The thermal radiation may be absorbed, reflected and transmitted when it falls onto an object, and there is the relationship among absorptivity  $\alpha$ , reflectivity  $\rho$  and transmissivity  $\tau$ :

$$\alpha + \rho + \tau = 1 \quad (2)$$

In temperature measurement, the effective radiation received by an IR camera includes three sections: the environmental radiation, thermal radiation of measured object and the radiation of atmospheric transmission. Camera IR detector combines the received radiant signal and then creates the corresponding signal  $f(T_r)$ :

$$f(T_r) = \tau_\alpha \varepsilon f(T) + \tau_\alpha (1 - \varepsilon) f(T_\mu) + (1 - \tau_\alpha) f(T_\alpha) \quad (3)$$

This is the general equation for temperature measurement in an IR camera, where  $\tau_\alpha$  is the transmissivity of atmosphere.  $T_r$  is the displayed temperature of camera,  $T$  is the surface temperature of object,  $T_\alpha$  is the atmosphere temperature and  $T_\mu$  is the environment temperature. In measurement temperature of blackbody surface, we have  $\varepsilon = 1$  and  $\tau_\alpha = 1$ , therefore  $f(T_r) = f(T)$  which is, the displayed temperature of camera is identical to the object's true temperature. But for other surface, especially the metals which have high reflectivity and low absorptivity, there is a significant difference between  $f(T_r)$  and  $f(T)$ , thus emissivity must be calibrated [17].

### 3. Experimental Procedures

Experiments on orthogonal cutting tests were performed on Aluminium alloy A7075-T6 thin-walled cylinders on a CNC turning centre (model TC50 Tabriz Co.). The experimental set-up is presented in Fig. 1. All cutting tests were performed using Sandvik PCD inserts (VCMW160404FP) in dry machining conditions. The influence of the machining process parameters such as cutting speed ( $V$ ), feed rate ( $F$ ), and depth of cut ( $A$ ) were studied. This experiment was designed using the full factorial design of experiments (DOE) technique. The different levels of test process parameters are presented in Table 1. A total of 27 experiments were designed and conducted, each with three replications to validate the results.

**Table 1. The different levels considered for each parameter.**

Cutting Parameter	Level			Unit
	1	2	3	
Cutting speed	230	350	470	m/min
Feed rate	60	120	180	mm/min
Depth of cut	0.75	1	1.25	mm

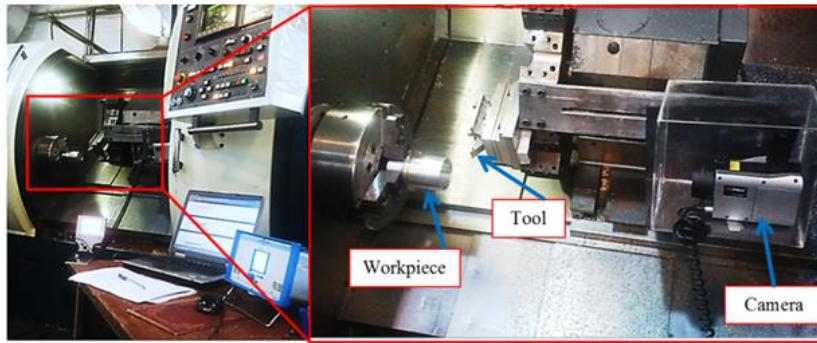


**Fig. 1. The experimental set-up.**

A thermal infrared camera (model DL700 made by Hi-Tech Resources) was used to measure the temperature during the machining process. The detector of camera was an uncool, Amorphous Silicon micro-bolometer with a sensitivity of  $0.08^{\circ}\text{C}$  at  $30^{\circ}\text{C}$ . Precise camera calibration and the determination of chip emissivity were necessary to increase the accuracy and certainty of the measurement. The camera was calibrated in a controlled temperature environment using a black body (model BBS-200 made by Optikos) with an emissivity coefficient of 0.994, independent of radiation wavelength. In order to find out chip emissivity, part of a chip was heated up to  $170^{\circ}\text{C}$  by a tungsten instrument. This makes the heat controllable through the application of specific current and voltage magnitudes. Since the aim of the present research is measuring the temperature of the chip, to increase the accuracy, the precise determination of the chip's emissivity in different temperature range is necessary. Therefore, a part of the chip, were heated to different temperatures ranging from  $50$  to  $310^{\circ}\text{C}$  by a tungsten element which makes a controllable heat via employing specified current and voltage. The accurate temperature of the chip was measured via a contact thermocouple (1 channel T/C Type -model 925-Testo) and the chip's temperature was measured via the thermal camera simultaneously. The inserted emissivity coefficient of the camera was determined and calibrated so that the measured temperature by camera was exactly the same as the measured temperature by thermocouple. Since during the experiments the reflection of the emitted radiation on the object in the measurement environment led to an increase in its emitted radiation, it follows that all light and heat sources in the measurement area were eliminated.

#### 4. ANN and ANFIS Architecture

Within artificial intelligence methods, ANN is the most commonly used model in engineering applications that deal with prediction, optimization, pattern recognition, and etcetera. Artificial neural networks work by detecting patterns in data, learning from the relations, and then adjusting to them. ANN is considered a processing system inspired by the performance of the human brain [18]. ANNs consist of a number of interconnected neurons. A neuron is an information-processing unit that receives several signals from its input links, each of which has a specific weight. Commonly, the initial weights of the network are set to random numbers. Thereafter corrections of the weights are performed from a set of training samples. The transfer function is a function used to transform the

activation level of a neuron into an output signal. The behaviour of an ANN model depends on both the weights and the activation function specified for the neuron. The mathematical model of the neuron shown in Fig. 2 tracks how signals are received, how they are then summed in the cell body, and how they are processed further so as to generate an output.

In order to find neuron input values, output from the connected neuron is multiplied by the synaptic strength of the connection between them. Equation 4 calculates the weighted sum of the input components  $x_i$ .

$$(net)_j = f(\sum_{i=1}^n w_{ij} x_i + b) \quad (4)$$

where,  $(net)_j$  is the output from the neuron,  $w_{ij}$  is connection's weight,  $b$  is the bias weight,  $n$  is the number of neurons in each layer, and  $f$  is the activation function.

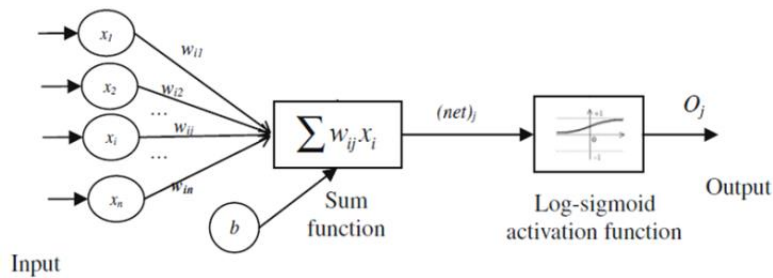


**Fig. 2. The mathematical model of the neuron.**

Neurons are structured depending on the learning algorithm used. An example of a learning algorithm is the back-propagation algorithm which is one of the most popular training methods used in ANN. This algorithm consists of at least three layers: an input layer, at least one hidden layer, and an output layer. The output from the input layer is connected as an input into the hidden layer. In a similar way, the output from the hidden layer is connected as an input into the output layer to produce the final output of the ANN. If there is a difference between actual and desired output patterns, the weights are adjusted to minimize this error and then propagated backwards through the network from the output layer to the input layer [19].

The type of neural network used in this study is a feed-forward back-propagation multi-layer perceptron (BPMLP) as shown in Fig. 3. Using the ANN model; the temperature value was predicted by using cutting speed, feed rate, and depth of cut values. The measured temperature was normalized as a 0 and 1 interval by using a standard min-max normalization technique. The results of 23 experiments of 27 designed tests were used to define the ANN model, and the 4 remaining tests were used to verify the results and test the ANN model. For learning purposes the data was divided into three sets: a training set consisting of 70% of the data, a validation set using 15% of the data, and a testing set using 15% of the data. The measured temperature was normalized as a 0 and 1 interval by using a standard min-max normalization technique.

The Levenberg-Marquardt algorithm is one of the best algorithms for training the ANN model with limited data [7-8]. The supervised learning method

implemented used a feed-forward back-propagation strategy with a Levenberg-Marquardt algorithm with the log-sigmoid used as activation function:

$$o_j = f(net)_j = \frac{1}{(1+e^{-(net)_j})} \quad (5)$$

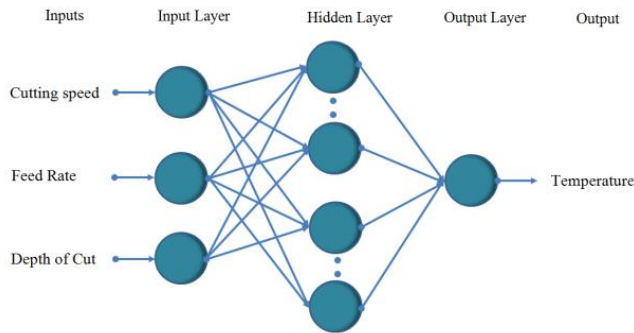


**Fig. 3. The structure of the ANN model.**

In order to determine the optimal architecture, different networks with different numbers of layers and neurons in the hidden layer were designed and tested. Using trial and error strategy to find the best model with high accuracy is one of the best methods in ANN model training especially when a hybrid model such as ANN-genetic model is not used [18]. Therefore, the number of neurons in the hidden layer was determined through a trial and error strategy. In the Fig. 4, the implemented strategy for finding the ANN model with the lowest error in predicting the temperature is shown. Several ANN model with one and two hidden layer and different number of neurons were investigated. As can be seen in the figure, the ANN model with one hidden layer and 12 neurons in the hidden layer performed best in predicting the temperature.

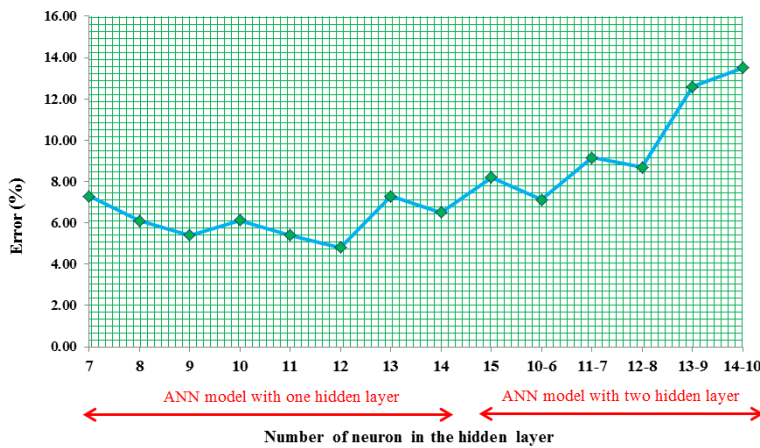


**Fig. 4. The error of the ANN models in predicting the temperature in terms of the number of neurons and hidden layer.**

Fuzzy sets were introduced by Zadeh [20], to represent and control data sets and information in which there are different alternative uncertainties. A decade later, he introduced fuzzy logic which is based on fuzzy set theory and represents an element with a certain degree of membership function usually taken as a real number between 0 and 1 [21]. In contrast to classical theory, where an element is either a member of the set or not, fuzzy logic is defined by linguistic terms rather than by numbers. Fuzzy inference systems (FIS) are one of the most well-known applications of fuzzy logic theory. The advantage of the fuzzy inference system is that it can deal with linguistic expressions and the advantage of a neural network is that it can be trained so it can learn and improve itself [22]. Jang takes advantage of strengths, combining the two techniques, and proposing the Adaptive Neuro-Fuzzy Inference System (ANFIS) [23]. The idea behind ANFIS is to design a system that uses a fuzzy system to represent knowledge in an interpretable manner. It has a learning ability derived from a neural network so it can adjust the membership function parameters as well as the linguistic rules directly from data. This enhances the system performance.

In other words, ANFIS is a graphical network demonstration of Sugeno-type fuzzy systems that is supported with ANN capabilities and is able to develop a network realization of “if-then” rules (Fig. 5).

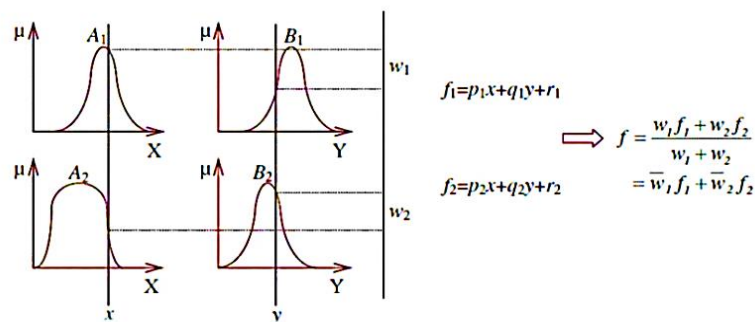


Fig. 5. First-order Sugeno fuzzy model.

If the rule base of ANFIS contains two fuzzy “if-then” rules of Sugeno-type fuzzy systems, equations of the rules can be described as follows:

$$\text{Rule 1: IF } x \text{ is } A_1 \text{ and } y \text{ is } B_1, \text{ THEN } f_1 = p_1x + q_1y + r_1 \quad (6)$$

$$\text{Rule 2: IF } x \text{ is } A_2 \text{ and } y \text{ is } B_2, \text{ THEN } f_2 = p_2x + q_2y + r_2 \quad (7)$$

The ANFIS architecture contains a five-layer feed forward neural network as shown in Fig. 6. Each ANFIS layer consists of several nodes which are described by the node function. The nodes in layers 1 and 4 are adaptive nodes which are represented as rectangles. Nodes in the layers 2, 3, and 5 are fixed nodes and are represented as circles. In the first layer each node constructs the membership grades of a linguistic label and implements a fuzzification. Node function can be described as:

$$o_i^1 = \mu_{A_i}(x) \quad (8)$$

where,  $(x)$  is the input to node  $i$ , and  $A_i$  is the linguistic label (fuzzy sets: small, large,) associated with this node function. In the second layer nodes calculate the firing weight of the rules and sends the product out. For example:

$$w_i = \mu_{A_i}(x) \times \mu_{B_i}(y), \quad i = 1,2 \tag{9}$$

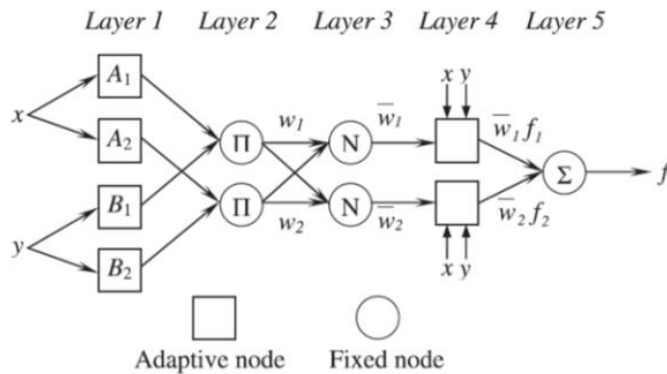


**Fig. 6. The ANFIS architecture.**

Each node output represents the firing weight of a rule. The third layer normalizes the membership functions by calculating the ratio of the  $i$ th rule’s firing weight to the sum of all rule’s firing weights:

$$\bar{w}_i = \frac{w_i}{(w_1+w_2)}, \quad i = 1,2 \tag{10}$$

The fourth layer computes the consequent parameters using a node function:

$$o_i^4 = \bar{w}_i(p_i x + q_i y + r_i) \tag{11}$$

where  $\bar{w}_i$  is the output of layer 3, and  $\{p_i, q_i, r_i\}$  is the parameter set.

Finally, the last layer calculates the overall output as the summation of all incoming signals, i.e.,

$$o_i^5 = \sum_i \bar{w}_i f_i = \frac{\sum_i w_i f_i}{\sum_i w_i} \tag{12}$$

The ANFIS procedure was described and explained in detail by Hassan et al. [24]. In this study, an ANFIS model was developed to predict temperature in the turning process. Three machining parameters, namely cutting speed, feed rate, and depth of cut were considered as input data. The measured temperature as output of the model was normalized as a 0 and 1 interval by using a standard min-max normalization technique. The experimental data were used to construct and train the ANFIS model. The experiments were divided into two groups. The first 16 experiments were used for training and the remaining was used for testing the ANFIS model. Several different models were developed by changing the training options in order to achieve satisfying results. The Gaussian functions were used to describe the membership degree of these variables. Gaussian membership function is one of the best algorithms for training ANFIS models especially when limited data is available [23, 24]. In addition, when training the ANFIS model, the Gaussian MF had the better result in comparison to the other function such as tri MF, dsig MF and gebll MF. After setting the initial parameter values in the ANFIS models, the input membership functions were adjusted using a hybrid learning technique.

## 5. Results and Discussion

All experimental machining tests were conducted as designed. In all tests, the temperature of the machining zone was measured using the infrared camera. The results are presented in Table 2 for all cutting conditions. Figure 7 represents the effect of three process parameters (cutting speed, feed rate, and depth of cut) on cutting zone temperature.

According to the results, an increase in any of the parameters of interest, (cutting speed, feed rate and, depth of cut) results in an increase in cutting zone temperature. As can be seen in Fig. 7 by increase the cutting speed, depth of cut and feed rate, the temperature is increased and the heat increase slope becomes steeper as the cutting speed rises in comparison to the depth of cut and feed rate. Analysis of the results shows that feed rate has a higher influence on temperature rise than depth of cut. This result is consistent and in accordance with other published works [2]. The highest measured temperature was 163°C and lowest was 84°C.

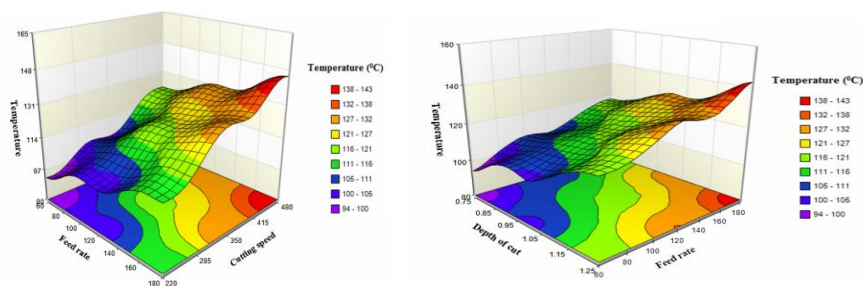


**Fig. 7.** The effect of the cutting speed, feed and depth of cut on temperature.

After conducting experimental tests and collecting and analysing the data, ANN and ANFIS models were developed in MATLAB. These models were utilized to predict the temperature (as detailed in section 4). Figure 8 shows the initial and final membership functions of the machining parameters that were derived by training the ANFIS model with the Gaussian function.

As can be seen, there is a considerable change in the final membership function of the cutting speed, with a large and small region reflecting considerable change and with smaller variation in the medium region. Results also show a distinctive change in the final membership function of the feed rate. However, the final membership function of depth of cut experienced a lower level of change in comparison with the other two parameters. By analysing the final membership functions, it can be concluded that cutting speed, feed rate, and depth of cut have the greatest impact on the measured temperature in turning, respectively. This result is consistent and in accordance with other published works [2].

In Fig. 9, measured temperature values during experiments were compared with predicted temperatures using ANN and ANFIS models by linear graphs. The graphs show that both models are capable of an accurate prediction of temperature in the cutting region. However, results show that predicted temperatures by ANFIS model are in closer agreement with experimental results. The advantage of the fuzzy inference system is that it can deal with linguistic expressions and the advantage of a neural network is that it can be trained so it

can learn and improve itself. The idea behind ANFIS is to design a system that uses a fuzzy system to represent knowledge in an interpretable manner. It has a learning ability derived from a neural network so it can adjust the membership function parameters as well as the linguistic rules directly from data. This enhances the system performance.

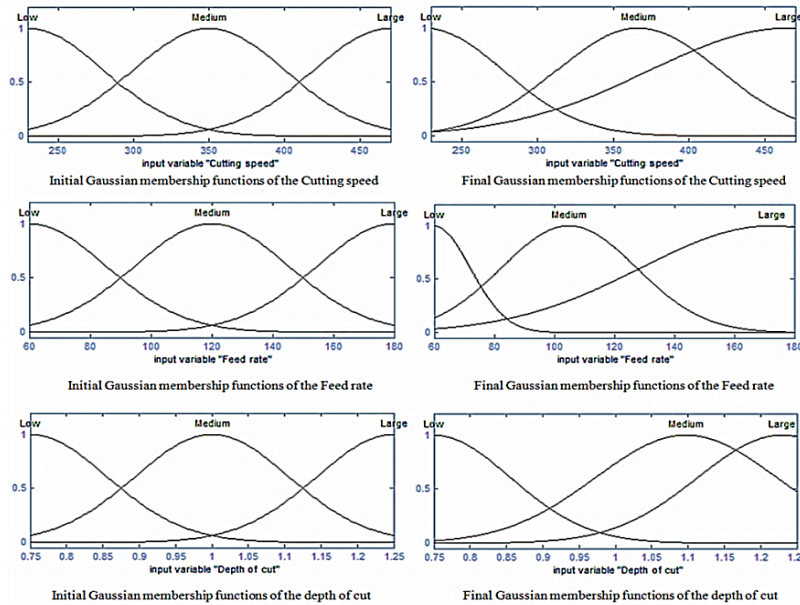


**Fig. 8. The Initial and final Gaussian MF of machining parameters.**

In Fig. 10, a scatter diagram is used in order to perform a detail analysis on the predicted results. The graph represents experimentally measured temperature values against predicted values using ANN and ANFIS models in a scatter format. R2 values (Correlation Coefficient) are 0.8978 for ANN model and 0.9594 for ANFIS model. This reveals the higher prediction accuracy of ANFIS model.

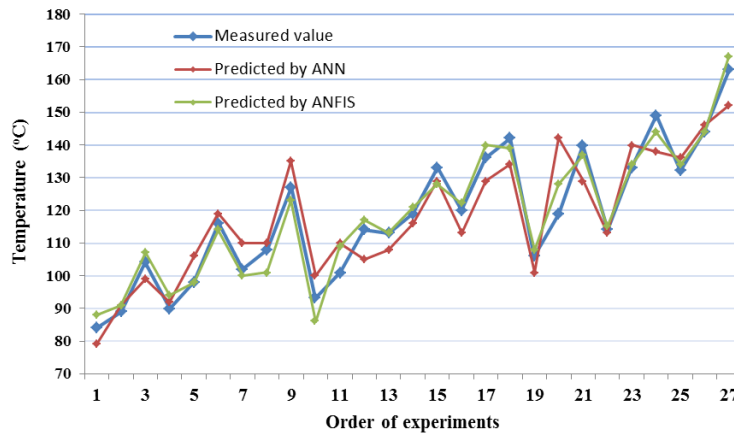


**Fig. 9. Comparison between predicted results of ANN and ANFIS models and measured values.**

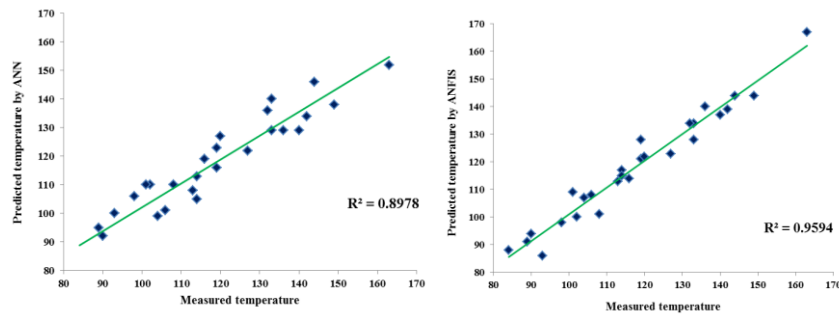


**Fig. 10. Scatter diagram of measured and predicted data using the ANFIS and ANN models.**

**Table 2. Machining experimental results.**

No	Cutting speed	Feed rate	Depth of cut	Temperature
1	230	60	0.75	84
2	230	60	1.00	89
3	230	60	1.25	104
4	230	120	0.75	90
5	230	120	1.00	95
6	230	120	1.25	116
7	230	180	0.75	102
8	230	180	1.00	108
9	230	180	1.25	127
10	350	60	0.75	93
11	350	60	1.00	96
12	350	60	1.25	114
13	350	120	0.75	113
14	350	120	1.00	108
15	350	120	1.25	133
16	350	180	0.75	120
17	350	180	1.00	121
18	350	180	1.25	142
19	470	60	0.75	106
20	470	60	1.00	111
21	470	60	1.25	140
22	470	120	0.75	114
23	470	120	1.00	121
24	470	120	1.25	149
25	470	180	0.75	132
26	470	180	1.00	137
27	470	180	1.25	163

As mentioned earlier, the results of 23 experiments of 27 designed tests were used to define the ANN model, and the 4 remaining tests were used to verify the results and test the model. Three other experiments were randomly selected to evaluate the mean error of the ANN model. The predicted temperatures by ANN and ANFIS for 7 experiments are presented in Table 3. Prediction errors were calculated using the Eq. (13):

$$\text{Error (percentage)} = \frac{\text{experimentally measured value} - \text{predicted value}}{\text{experimentally measured value}} \quad (13)$$

According to the results provided in Table 3, mean error values of the seven sample experiments for ANN and ANFIS models were 5.30 and 2.82 respectively. Even though the results obtained by ANN model are accurate enough, the ANFIS model reflect less error, and is therefore better at accurately predicting temperature.

**Table 3. Average predicted error by ANN and ANFIS model.**

No	Cutting speed	Feed rate	Depth of cut	Measured temperature	Predicted temperature by ANN	Predicted temperature by ANFIS	ANN error	ANFIS error
1	230	60	0.75	84	79	88	5.95	4.76
2	230	180	1.25	127	135	123	6.29	3.14
3	350	120	1	119	116	121	2.52	1.68
4	350	180	1.25	142	134	139	5.63	2.11
5	470	60	0.75	106	101	108	4.71	1.88
6	470	120	1	133	140	134	5.26	0.75
7	470	180	1.25	163	152	167	6.74	5.45
Average error in the above experiments							5.30	2.82
Average error in the all 27 experiments							5.83	3.17

## 6. Conclusion Remarks

In this article, the effect of machining process parameters on temperature change in the cutting region is investigated using ANN and ANFIS models to predict the temperatures. In the first step, the effect of the machining process parameters including cutting speed, feed rate, and depth of cut were measured over the cutting zone and the temperature was evaluated by designing and conducting 27 machining experimental tests. The temperature was measured using an infrared camera. The next step involved training ANN and ANFIS models using experimentally collected data and studying their ability to accurately predict temperature. Analysis of the results show that ANFIS predicts cutting zone temperatures with higher accuracy, as the prediction error associated with ANFIS model was only 3.17% comparing to 5.83% for ANN model. The ANFIS models in general are more accurate than ANN in modelling manufacturing processes and reflect the benefits of combining fuzzy systems capabilities with neural networks.

## References

1. Cotterell, M.; Ares, E.; Yanes, J.; López, F.; Hernandez, P.; and Peláez, G. (2013). Temperature and strain measurement during chip formation in orthogonal cutting conditions applied to Ti-6Al-4V. *Procedia Engineering*, 63, 922-930.
2. Masoudi, S.; Amirian, G.; Saeedi, E.; and Ahmadi, M. (2015). The effect of quench-induced residual stresses on the distortion of machined thin-walled parts. *Journal of Materials Engineering and Performance*, 24(10), 3933-3941.

3. Heigel, J.C.; Whitenon, E.; Lane, B.; Donmez, M. A.; Madhavan, V.; and Moscoso-Kingsley, W. (2017). Infrared measurement of the temperature at the tool-chip interface while machining Ti-6Al-4V. *Journal of Materials Processing Technology*, 243, 123-130.
4. Masoudi, S.; Gholami, M. A.; Iariche, J. M.; Vafadar, A. (2017). Infrared temperature measurement and increasing infrared measurement accuracy in the context of machining process. *Advances in Production Engineering & Management*, 12(4), 353-362.
5. Chandrasekaran, M.; Muralidhar, M.; Krishna, C.M.; and Dixit, U.S. (2010). Application of soft computing techniques in machining performance prediction and optimization: a literature review. *The International Journal of Advanced Manufacturing Technology*, 46(5-8), 445-464.
6. Rangwala, S.S.; and Dornfeld, D.A. (1989). Learning and optimization of machining operations using computing abilities of neural networks. *IEEE Transactions on Systems, Man, and Cybernetics*, 19(2), 299-314.
7. Rai, J.K.; Villedieu, L.; and Xirouchakis, P. (2008). Mill-cut: a neural network system for the prediction of thermo-mechanical loads induced in end-milling operations. *The International Journal of Advanced Manufacturing Technology*, 37(3-4), 256-264.
8. Korkut, I.; Acir, A.; and Boy, M. (2011). Application of regression and artificial neural network analysis in modelling of tool-chip interface temperature in machining. *Expert Systems with Applications*, 38(9), 11651-11656.
9. Azouzi, R.; and Guillot, M. (1997). On-line prediction of surface finish and dimensional deviation in turning using neural network based sensor fusion. *International Journal of Machine Tools and Manufacture*, 37(9), 1201-1217.
10. Kohli, A.; and Dixit, U.S. (2005). A neural-network-based methodology for the prediction of surface roughness in a turning process. *The International Journal of Advanced Manufacturing Technology*, 25(1-2), 118-129.
11. Quiza, R.; Figueira, L.; and Davim, J.P. (2008). Comparing statistical models and artificial neural networks on predicting the tool wear in hard machining D2 AISI steel. *The International Journal of Advanced Manufacturing Technology*, 37(7-8), 641-648.
12. Aydın, M.; Karakuzu, C.; Uçar, M.; Cengiz, A.; and Çavuşlu, M.A. (2013). Prediction of surface roughness and cutting zone temperature in dry turning processes of AISI304 stainless steel using ANFIS with PSO learning. *The International Journal of Advanced Manufacturing Technology*, 67(1-4), 957-967.
13. Madić, M. I. L. O. Š.; and Radovanović, M. I. R. O. S. L. A. V. (2012). An artificial intelligence approach for the prediction of surface roughness in CO2 laser cutting. *Journal of Engineering Science and Technology*, 7(6), 679-689.
14. Azmi, A.I. (2015). Monitoring of tool wear using measured machining forces and neuro-fuzzy modelling approaches during machining of GFRP composites. *Advances in Engineering Software*, 82, 53-64.
15. Hamza, R.M.A. (2011). Multi-objective neural network modelling for improving stud arc welding process joining. *Journal of Engineering Science and Technology*, 6(3), 382-391.

16. Valiorgue, F.; Brosse, A.; Naisson, P.; Rech, J.; Hamdi, H.; and Bergheau, J. M. (2013). Emissivity calibration for temperatures measurement using thermography in the context of machining. *Applied Thermal Engineering*, 58(1), 321-326.
17. Yanming, Q.U. A.N.; Hao, X.U.; and Zhiyong, K.E. (2011). Research on some influence factors in high temperature measurement of metal with thermal infrared imager. *Physics Procedia*, 19, 207-213.
18. Karayiannis, N.; and Venetsanopoulos, A.N. (2013). *Artificial neural networks: learning algorithms, performance evaluation, and applications*, (Vol. 209). Springer Science and Business Media.
19. Wang, S.C. (2003). *Artificial neural network. In Interdisciplinary computing in java programming*. Springer US.
20. Zadeh, L.A. (1965). Fuzzy sets. *Information and Control*, 8(3), 338-353.
21. Zadeh, L.A. (1975). The concept of a linguistic variable and its application to approximate reasoning—I. *Information sciences*, 8(3), 199-249.
22. Wang, J.S.; and Lee, C.G. (2002). Self-adaptive neuro-fuzzy inference systems for classification applications. *IEEE Transactions on Fuzzy Systems*, 10(6), 790-802.
23. Jang, J.S.R.; Sun, C.T.; Mizutani, E.; and Ho, Y.C. (1998). Neuro-fuzzy and soft computing-a computational approach to learning and machine intelligence. *Proceedings-IEEE Transactions on Automatic Cotrol*, 86(3), 600-603.
24. Hassan, S.; Khanesar, M.A.; Kayacan, E.; Jaafar, J.; and Khosravi, A. (2016). Optimal design of adaptive type-2 neuro-fuzzy systems: A review. *Applied Soft Computing*, 44, 134-143.